Critical behavior in $N_t = 4$ staggered fermion thermodynamics

Claude Bernard
Department of Physics, Washington University, St. Louis, Missouri 63130

Carleton DeTar
Department of Physics, University of Utah, Salt Lake City, Utah 84112

Steven Gottlieb
Indiana University, Bloomington, Indiana 47405

Urs M. Heller
SCRI, The Florida State University, Tallahassee, Florida 32306-4130

James Hetrick
University of the Pacific, Stockton, California 95211

Kari Rummukainen
NORDITA, Blegdamsvej 17, DK-2100 Copenhagen Ø, Denmark

Robert L. Sugar
Department of Physics, University of California, Santa Barbara, California 93106

Doug Toussaint
Department of Physics, University of Arizona, Tucson, Arizona 85721

Quantum chromodynamics with two zero mass flavors is expected to exhibit a phase transition with O(4) critical behavior. Fixing the universality class is important for phenomenology and for facilitating the extrapolation of simulation data to physical quark mass values. Other groups have reported results from lattice QCD simulations with dynamical staggered quarks at $N_t = 4$, which suggest a departure from the expected critical behavior. We have pushed simulations to the largest volumes and smallest quark mass to date. Strong discrepancies in critical exponents and the scaling equation of state persist.

PACS number(s): 12.38.Gc, 11.30.Rd, 12.38.Aw, 12.38.Mh

I. INTRODUCTION

It is generally expected that two-flavor QCD undergoes a high temperature chiral-symmetry-restoring phase transition at zero quark mass with O(4) critical behavior [1]. Should the axial anomaly disappear simultaneously with the phase transition, the Pisarski-Wilczek scenario then suggests a fluctuation-driven first order phase transition. Verifying these expectations is important for understanding the phenomenology of the transition and for facilitating an extrapolation of simulation data to physical quark masses. Since the staggered fermion scheme breaks the anomaly explicitly at nonzero lattice spacing, lattice QCD at fixed N_t with staggered fermions, as a statistical system in its own right, is similarly expected to exhibit at least O(2) universality, with O(4) or a fluctuation-driven first-order phase transition emerging in the continuum limit $N_t \to \infty$. At $N_t = 4$ the lattice spacing is coarse enough that, if there is a critical point at zero quark mass, O(2) is the only likely option.

The standard test of universality compares critical exponents. Comparing the critical scaling function itself gives further insight. To test for the expected universality we use the standard correspondence between QCD variables and O(N) spin variables, which identifies quark mass m_q/T with magnetic field h, inverse gauge coupling $6/g^2$ with temperature $T/T_c(0)$, chiral condensate $\langle \bar{\psi}\psi \rangle$ with magnetization M, and the action (plaquette) with the energy density. A critical point is expected to occur at zero quark mass and nonzero coupling $6/g^2(0)$. For studies at fixed N_t, therefore, we define [2]

$$h = a m_q N_t$$

$$t = 6/g^2 - 6/g_c^2 \propto T/T_c - 1. \qquad (1)$$

Critical scaling theory predicts that for small quark masses we have the Fisher scaling relation [3]

$$\langle \bar{\psi}\psi \rangle h^{-1/\delta} = f_{\text{QCD}}(x) = c_y f_G(c_x x) \qquad (2)$$

where $x = t h^{-1/\beta\delta}$, c_x and c_y are scale constants, $f_{QCD}(x)$ is the critical scaling function for QCD and $f_G(x)$ is that for the appropriate universality class G. Only the scale constants c_x and c_y are adjustable. Some critical exponents are given in Table I. Outside the Ginzburg scaling region, by definition, there are appreciable nonleading, nonscaling contributions to

TABLE I. Some critical exponents in three dimensions.

	y_t	y_h	δ	β
MF	1.5	2.25	3	0.5
$O(2)$	1.495	2.484	4.81	0.3455
$O(4)$	1.337	2.487	4.851	0.3836
$Z(2)$	1.61	2.5	5.0	0.31

$\langle \bar{\psi}\psi \rangle$, analytic in t and h. In addition to corrections analytic in t and h, there are correction terms with subleading exponents, universal and nonanalytic in t and h. The mean-field scaling function is known exactly. For the O(4) scaling function we use results of a numerical simulation [4].

There is a similar scaling relation for the energy density. In QCD the energy density (plaquette) is dominated by gluon degrees of freedom, which are indirectly affected by the chiral singularity. So apparently there is a much larger analytic contribution. Consequently, we have found the plaquette observable much less useful for testing critical scaling. Here we concentrate on the scaling of $\langle \bar{\psi}\psi \rangle$.

In the next section we discuss an analysis of finite size effects, present a determination of some critical exponents, and compare our results with the critical scaling function. In the concluding section we suggest reasons for the discrepancies observed. A preliminary version of this study was presented at Lattice '97 [5].

II. ANALYSIS OF CRITICAL BEHAVIOR

Our data set extends an old sample on lattice sizes $L^3 \times N_t$ with $N_t = 4, L = 8$ and quark masses $am_q = 0.025$ and 0.0125, which was generated with the standard one-plaquette gauge action plus two-flavor staggered fermion action. Our new simulations decrease the quark mass to $am_q = 0.008$ and increase the spatial lattice size L to 24 (aspect ratio 6). We also reanalyzed old data at $N_t = 6$, 8, and 12 [6]. The old data, unfortunately, are limited to aspect ratio $L/N_t = 2$. The extent of our $N_t = 4$ data sample is given in Table II. Included in this table are values for global observables. For equilibration we typically dropped the first 300 molecular dynamics time units of each run.

Over the range of nonzero quark masses considered, there

TABLE II. Parameters in $N_t = 4$ data set and two global observables. Run and step lengths are in molecular dynamics time units.

| L	am_q	$6/g^2$	Step	Length	Plaquette	$\langle \bar{\psi}\psi \rangle$
12	0.008	5.25	.003	1965	1.455(2)	0.346(4)
12	0.008	5.255	.003	2200	1.467(4)	0.320(11)
12	0.008	5.26	.003	2130	1.506(6)	0.20(2)
12	0.008	5.265	.003	2170	1.512(4)	0.18(2)
12	0.008	5.27	.003	2045	1.532(2)	0.116(7)
12	0.008	5.28	.003	1965	1.5466(8)	0.075(2)
12	0.0125	5.25	.005	2920	1.4515(10)	0.364(2)
12	0.0125	5.26	.005	4630	1.467(2)	0.335(5)
12	0.0125	5.27	.005	7320	1.498(3)	0.254(11)
12	0.0125	5.28	.005	2820	1.5383(15)	0.129(5)
12	0.025	5.27	.01	2150	1.4652(9)	0.370(2)
12	0.025	5.28	.01	2075	1.483(2)	0.335(5)
12	0.025	5.29	.01	1975	1.512(4)	0.268(10)
16	0.008	5.255	.003	2460	1.4673(10)	0.321(3)
16	0.008	5.26	.003	1445	1.494(5)	0.24(2)
16	0.008	5.265	.003	1825	1.520(3)	0.155(12)
16	0.008	5.27	.003	1310	1.5346(8)	0.105(3)
16	0.0125	5.27	.005	4700	1.500(4)	0.251(13)
16	0.0125	5.275	.005	4900	1.530(2)	0.153(6)
24	0.008	5.255	.003	950	1.4656(8)	0.326(2)
24	0.008	5.26	.003	1698	1.484(2)	0.276(5)
24	0.008	5.263	.003	1703	1.507(2)	0.202(8)
24	0.008	5.265	.003	1702	1.5238(12)	0.140(5)
24	0.008	5.27	.003	1700	1.5350(5)	0.104(2)
24	0.0125	5.265	.005	1950	1.4747(6)	0.3208(15)
24	0.0125	5.268	.005	1760	1.487(2)	0.288(6)
24	0.0125	5.27	.005	3126	1.502(2)	0.243(7)
24	0.0125	5.272	.005	1760	1.5198(13)	0.186(5)
24	0.0125	5.275	.005	1950	1.5295(11)	0.155(4)
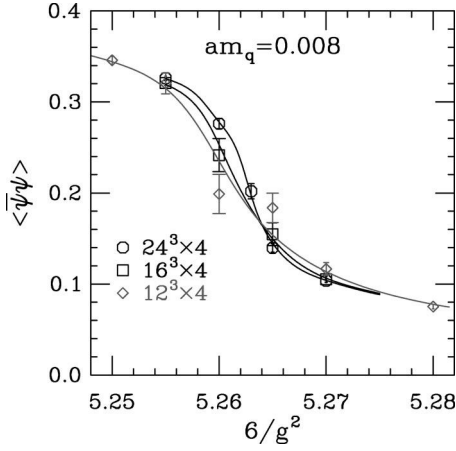
FIG. 1. Order parameter vs inverse gauge coupling for various lattice sizes for $am_q=0.008$. Curves show results from reweighting the data sample.

appears to be no phase transition—only a crossover, as illustrated for $am_q=0.008$ in Fig. 1. Evidently, however, the crossover steepens as the lattice volume is increased. The crossover, or ''pseudo-critical point'' is signaled by a peak in a susceptibility for any lattice size. For example the mixed plaquette-chiral condensate susceptibility, corresponding to the slope in Fig. 1,

$$\chi_{mt}=\frac{\partial\langle\bar{\psi}\psi\rangle}{\partial(6/g^2)}, \tag{3}$$

is plotted in Fig. 2 for the $16^3\times4$ lattice. Here, as well as in Fig. 1, we use multihistogram reweighting to interpolate the data from the simulation points and locate the peak. The error analysis was performed with the jackknife method, which enables us to obtain reliable error estimates for both the peak height and location.

The peak location (crossover coupling $6/g_{pc}^2$) shows little variation in lattice size for $L>8$. For example the peak location in χ_{mt} shifts from 5.2605(10) to 5.2623(6) as L in-
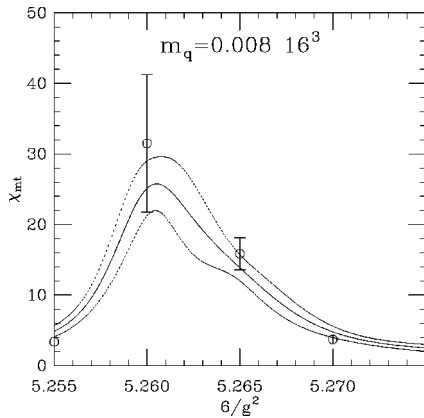

FIG. 2. The mixed $\langle\bar{\psi}\psi\rangle$-plaquette susceptibility χ_{mt} as a function of inverse coupling $6/g^2$ for $am_q=0.008$ on a $16^3\times4$ lattice. Curves show results from reweighting together with one-standard-deviation bootstrap errors.
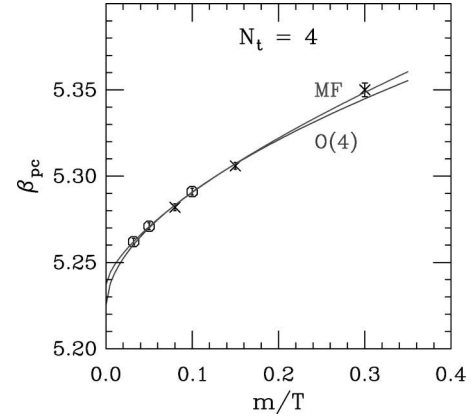

FIG. 3. Trajectory of the pseudocritical point $6/g_{pc}^2$ as a function of quark mass in units of temperature m_q/T for $N_t=4$. Crosses indicate points from Karsch and Laermann [2]. Also shown are fits to both mean-field (upper curve) and $O(4)$ (lower curve) scaling predictions.

creases from 12 to 24, a scarcely significant change. It also shows little variation among the susceptibilities chosen. For example the peak location varies by ±0.001 over the susceptibilities considered. In all cases we take the result from the largest volume and assign an error of 0.002. Close to the critical point the peak position occurs at a fixed value of the scaling variable $x=x_{pc}$, so we have the scaling relation [2]

$$6/g_{pc}^2=6/g_{pc}(0)^2+x_{pc}(am_qN_t)^{1/\delta\beta}. \tag{4}$$

Shown in Fig. 3 is the trajectory of the pseudocritical point, fitted to both $O(4)$ and mean-field predictions. Both fits are good. An $O(2)$ fit would do equally well. Such agreement was first found by Karsch and Laermann and inspired hope that the simulations had entered the scaling region [2].

Problems with scaling were uncovered in studies at larger volumes [7–9]. In Figs. 4 and 5 we plot the peak height of the χ_{mt} susceptibility for two fixed quark masses. The increase in peak height with increasing volume reflects the
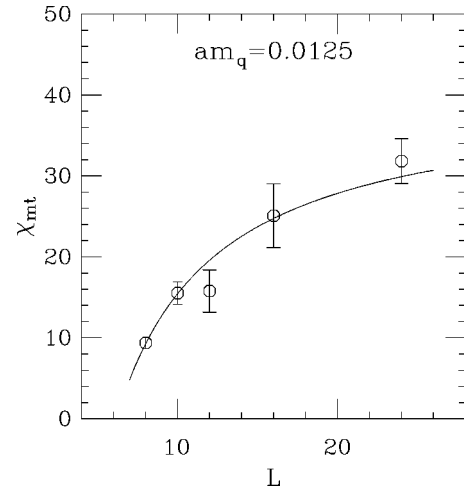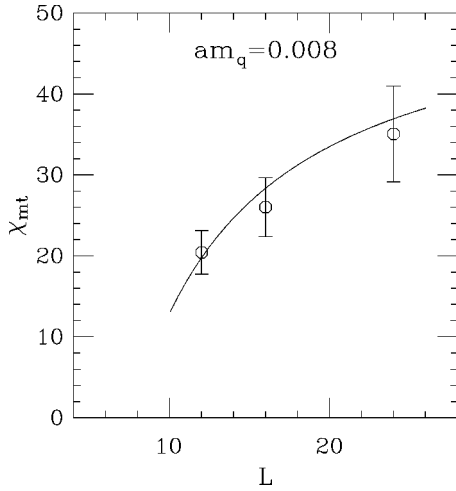

FIG. 4. Finite size analysis of the peak height in the mixed $\langle\bar{\psi}\psi\rangle$-plaquette susceptibility χ_{mt} at $am_q=0.0125$ for $N_t=4$.

FIG. 5. Same as Fig. 4, but for $am_q = 0.008$.

steepening trend seen, for example, in Fig. 1. It is necessary to extrapolate to infinite volume at each quark mass before checking scaling. We start by assuming the conventional scenario, in which the critical point occurs at $am_q = 0$. Then at nonzero mass, the susceptibility has a finite limit at large volume. We make an *ad hoc* choice for an extrapolation formula with the result shown in Figs. 4 and 5.

$$\chi_{mt}^{\max}(L) = \chi_{mt}^{\max}(\infty) + b/L. \tag{5}$$

The $am = 0.0125$ data covers the largest range of lattice sizes. Varying the inverse power of L from 1/2 to 1 to 2 gives a slight preference for $1/L$ at this mass. Given the uncertainties in the values themselves, we feel it is safe to use any of these extrapolations, and we have chosen $1/L$ for all masses.
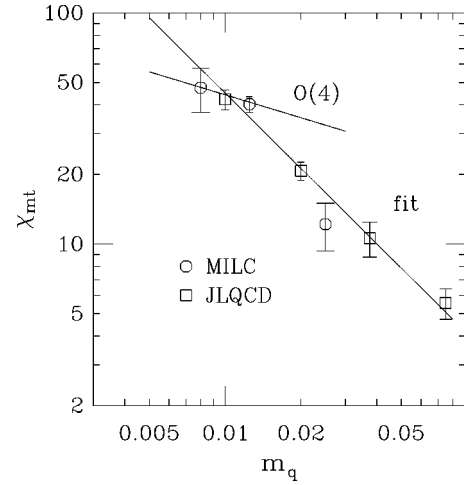
The extrapolated peak height of the χ_{mt} susceptibility is expected to scale with decreasing quark mass. For this susceptibility, the expected scaling relation is

$$\chi_{mt}^{\max} \sim (am_q)^{(\beta-1)/\beta\delta}. \tag{6}$$

We compare this prediction with results from our analysis in Fig. 6. Also shown are similarly extrapolated JLQCD values [9]. If we include all points in the fit, the scaling exponent is $-1.08(8)$, compared with an $O(4)$ prediction of -0.33—a clear disagreement, corroborating results of the JLQCD and Bielefeld groups [7–9]. However, it is evident in Fig. 6 that at the three lightest masses this observable alone does not exclude $O(4)$. To test sensitivity to our extrapolation formula, we carried out the same analysis, replacing $1/L$ by $1/\sqrt{L}$ and $1/L^2$. The resulting scaling exponents are $-1.24(11)$ and $-0.94(5)$, respectively, still clearly at variance with $O(4)$ over the full mass range studied.

A similar fit of the plaquette susceptibility, $\chi_{tt} = \partial\langle\Box\rangle/\partial(6/g^2)$, also including $1/L$-extrapolated JLQCD results, yields a scaling exponent of $-0.78(7)$, while the $O(4)$ prediction is $1/\delta - 2/(\delta\beta) + 1 = 0.13$. The $1/\sqrt{L}$ and $1/L^2$ extrapolations give $-0.95(10)$ and $-0.64(5)$, respectively.

Because the crossover steepens so much with increasing lattice volume and small quark mass, it is worthwhile look-

FIG. 6. Scaling analysis of extrapolated peak height for the mixed $\langle\bar{\psi}\psi\rangle$-plaquette susceptibility χ_{mt} for $N_t = 4$. Results from Ref. [9] are obtained by similar infinite volume extrapolation. Also shown is the $O(4)$ scaling prediction.

ing for evidence for two-phase metastability, signaling a first-order phase transition. Figure 7 shows the simulation time histories of our runs at $am_q = 0.008$. While we certainly see long correlation times, we see no evidence for a first order transition in these histories. In Fig. 8 we show time histories from hot and cold starts at $am_q = 0.0125$ (two hot and two cold starts) and $am_q = 0.008$ at values of $6/g^2$ near the peaks of the susceptibilities. Again, there is no evidence for a first order transition.

We turn next to an analysis of the critical scaling function, given by Eq (2). Here, again, we assume that we are in the scaling region. The analysis then depends on which critical exponents we adopt. Using $O(4)$ critical exponents from Kanaya and Kaya [10], we construct $f_{\mathrm{QCD}}(x)$ and compare with the scaling function $f_{O(4)}(x)$ for $O(4)$ [4] in Fig. 9. Essentially all of the data lie at positive x, which permits a
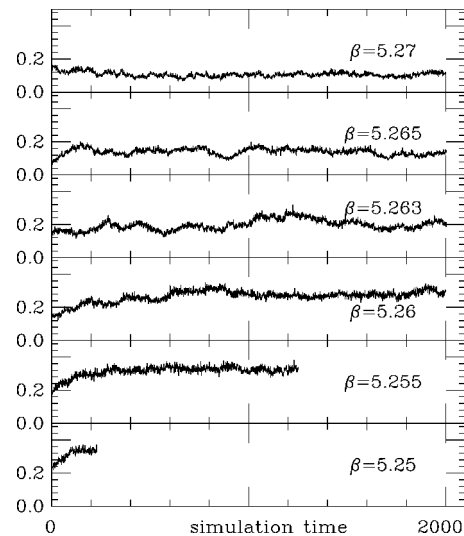
FIG. 7. Simulation time history of the order parameter $\langle\bar{\psi}\psi\rangle$ near the crossover for the largest volume $24^3\times4$.
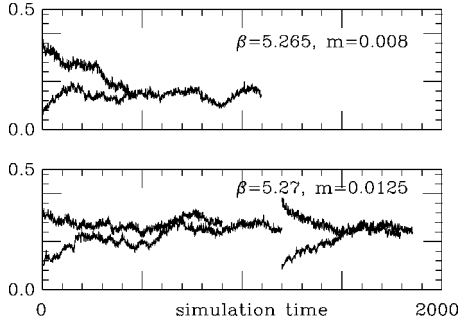
FIG. 8. Same as Fig. 7 showing evolution from hot and cold starts at or near the crossover. In each case the initially upper (lower) trace follow a cold (hot) start.

log-log plot. Vertical and horizontal displacements of the log-log scaling curves correspond to adjusting c_x and c_y. Clearly, no such displacement would result in good agreement. The newer data are plotted with octagons and squares. We observe: (1) The QCD curve falls with increasing steepness as the quark mass is decreased. Since the slope of the curve at the crossover gives the peak height of the χ_{mt} susceptibility, the disagreement there is consistent with the observed lack of scaling of the peak height itself. (2) The new data at larger volume and smaller quark mass show generally worse agreement with the $O(4)$ scaling curve. (3) The crossover regions, indicated in the QCD results by line segments and in the $O(4)$ scaling function by a dashed line, are far from agreeing.

We show a similar comparison of the QCD scaling function with the mean-field prediction in Fig. 10. Again the disagreement is significant. Although we have not measured the $O(2)$ scaling function, so cannot make a direct comparison, given the close similarity of the critical exponents with $O(4)$, we do not expect any improvement with that choice.

We conclude that if the $N_t=4$ theory falls in the $O(2)$ or $O(4)$ universality class, simulations at present masses do not reach the critical scaling region. Furthermore, as the quark
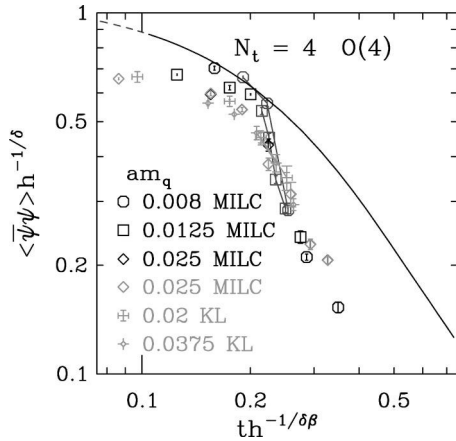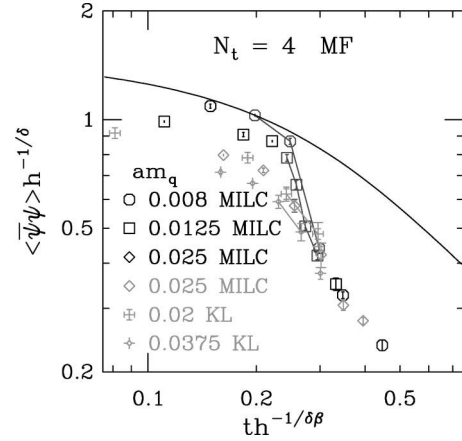

FIG. 10. Same as Fig. 9 but with mean field exponents and the mean field scaling function.

mass is decreased over the present range, disagreement with scaling predictions worsens, offering little hope that we might be getting closer.

A similar analysis at larger N_t is shown in Fig. 11. Perhaps there is improvement with increasing N_t. However, our $N_t=12$ sample includes data only at a single quark mass, making it the weakest test. Furthermore, for $N_t>4$ we have no results for $L>2N_t$, where we first encountered difficulties at $N_t=4$.

III. DISCUSSION AND SPECULATIONS

We have seen that new simulations at smaller quark mass and larger volume at $N_t=4$ have raised doubts about the extent of the previously observed agreement between QCD and $O(4)$ [2,6]. The conventional staggered fermion action with the conventional choice of scaling variables does not show good agreement with the $O(4)$ or mean field scaling functions at present quark masses and temperatures. (Wilson
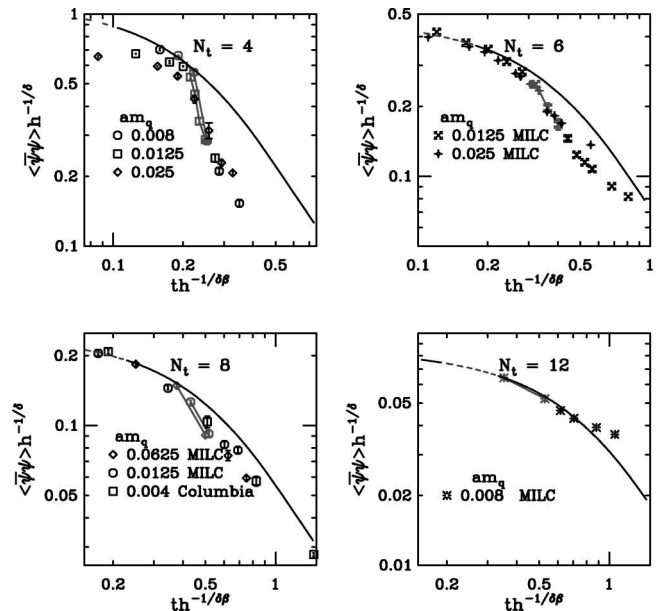

FIG. 9. Scaling test at $N_t=4$ of the order parameter $\langle \bar{\psi}\psi \rangle$, based on $O(4)$ critical exponents. Shown for comparison is the $O(4)$ scaling function from Ref. [4]. The crossover region is indicated by line segments in the data and a dashed line in the $O(4)$ scaling function.

FIG. 11. Same as Fig. 9 but for $N_t=4,6,8,$ and 12.

quarks with an improved gauge action seem to behave very differently [11].)

Believers in the conventional sigma model scenario could argue that the critical region is attained only when π and σ correlation lengths are considerably greater than $1/T_c$. Only in that case is the reduction of QCD to a three-dimensional sigma model well justified. Here, typically, these correlation lengths are smaller than $1/T_c$. Still, the observed worsening of the agreement with decreasing quark mass is disturbing.

Recent results from simulations of the conventional $N_t = 4$ staggered fermion action, augmented by a four-fermi term (''chiral QCD'') permit another speculation [12]. With the additional four-fermi interaction, Kogut, Lagaë, and Sinclair are able to carry out simulations at precisely zero quark mass. They find evidence for a first order phase transition at small four-fermi coupling. A nearby first order phase transition could spoil the approach to the critical point. Indeed, one cannot, therefore, rule out the possibility that the first order phase transition extends to zero four-fermion coupling for a small range of quark masses below the reach of our

simulations. In this case, one expects a critical end point at a nonzero quark mass m_{qc} in the Ising or mean-field universality class. At $N_t = 6$ the same group finds evidence for a crossover instead of a first-order phase transition [13]. Thus, one may speculate that the conventional one-plaquette, staggered fermion action at $N_t = 4$ is plagued by lattice artifacts large enough to obliterate the expected $am_q = 0$ critical point, but these artifacts diminish at higher N_t.

[1] R. Pisarski and F. Wilczek, Phys. Rev. D **29**, 338 (1984).
[2] F. Karsch and E. Laermann, Phys. Rev. D **50**, 6954 (1994).
[3] D.J. Amit, *Field Theory, the Renormalization Group, and Critical Phenomena* (McGraw-Hill, New York, 1978).
[4] D. Toussaint, Phys. Rev. D **55**, 362 (1997).
[5] C. Bernard, Nucl. Phys. B (Proc. Suppl.) **63**, 400 (1998).
[6] C. Bernard, Phys. Rev. D **54**, 4585 (1996).
[7] A. Ukawa, Nucl. Phys. B (Proc. Suppl.) **53**, 95 (1997).
[8] G. Boyd, F. Karsch, E. Laermann, and M. Oevers, talk given at 10th International Conference on Problems of Quantum Field Theory, Alushta, Ukraine, 1996, hep-lat/9607046.

[9] JLQCD Collaboration, S. Aoki *et al.*, Phys. Rev. D **57**, 3910 (1998).
[10] K. Kanaya and S. Kaya, Phys. Rev. D **51**, 2404 (1995).
[11] Y. Iwasaki, K. Kanaya, S. Kaya, and T. Yoshie, Phys. Rev. Lett. **78**, 179 (1997); S. Aoki, Y. Iwasaki, K. Kanaya, S. Kaya, A. Ukawa, and T. Yoshié, Nucl. Phys. B (Proc. Suppl.) **63**, 397 (1998).
[12] J. Kogut, J.-F. Lagaë, and D.K. Sinclair, Phys. Rev. D **58**, 034504 (1998).
[13] J. Kogut, J.-F. Lagaë, and D.K. Sinclair, Nucl. Phys. B (Proc. Suppl.) **73**, 471 (1999).